Neuron, Vol. 40, 177–188, September 25, 2003, Copyright ©2003 by Cell Press

Dynamics of Population Code for Working Memory in the Prefrontal Cortex

E.H. Baeg,[1] Y.B. Kim,[1] K. Huh,[2]
I. Mook-Jung,[3] H.T. Kim,[4] and M.W. Jung[1,3,*]
[1]Neuroscience Laboratory
Institute for Medical Sciences
[2]Department of Neurology and
[3]Brain Disease Research Center
Ajou University School of Medicine
Suwon 442-721
[4]Department of Psychology
Korea University
Seoul 136-701
Korea

Summary

Some neurons (delay cells) in the prefrontal cortex elevate their activities throughout the time period during which the animal is required to remember past events and prepare future behavior, suggesting that working memory is mediated by continuous neural activity. It is unknown, however, how working memory is represented within a population of prefrontal cortical neurons. We recorded from neuronal ensembles in the prefrontal cortex as rats learned a new delayed alternation task. Ensemble activities changed in parallel with behavioral learning so that they increasingly allowed correct decoding of previous and future goal choices. In well-trained rats, considerable decoding was possible based on only a few neurons and after removing continuously active delay cells. These results show that neural activity in the prefrontal cortex changes dynamically during new task learning so that working memory is robustly represented and that working memory can be mediated by sequential activation of different neural populations.

Introduction

Working memory refers to the short-lasting memory buffer of the brain that represents the current content of ongoing conscious mental operations (Baddeley, 1986). Delay tasks, such as delayed response and delayed alternation tasks, have been widely used for the study of working memory. An essential nature of these tasks is the temporal gap (delay period) between a sensory cue (or previous response) and a subsequent behavioral response, during which a retrospective memory (RM) of the presented cue (or previous response) or a prospective memory (PM) of the future behavioral choice should be maintained in order to yield a correct response. Behavioral studies have shown that damage in the prefrontal cortex (PFC) impairs performance in these tasks across various mammalian species (Kolb, 1990; Fuster, 1997), indicating that the PFC plays an essential role in working memory. Physiological studies have found neurons in the PFC with elevated activities throughout the delay period (delay cells) (Fuster and Alexander, 1971; Kubota and Niki, 1971; Funahashi et al., 1989; Miller et al., 1996), suggesting that working memory is mediated by continuous activities of PFC neurons. In support of this suggestion, subsequent modeling studies have shown that RM can be maintained by persistent neuronal activity based on synaptic reverberation in a recurrent circuit (see Wang, 2001, for review). These studies have led to the current prevailing view that persistent neuronal activity in the PFC plays an essential role in mediating working memory (Goldman-Rakic, 1995; Fuster, 1997; Funahashi, 2001; Miller and Cohen, 2001; Wang, 2001).

The recent development of multiple single neuron recording techniques has facilitated real-time monitoring of ensemble neuronal activities, providing valuable insights into the neural basis of various brain functions (e.g., Wilson and McNaughton, 1993; Jog et al., 1999; Laubach et al., 2000). Few studies have examined neuronal ensemble activities in the PFC, however (Chang et al., 2000). Ensemble recording would be particularly valuable in elucidating neural mechanisms of PFC functions, because the following factors make reconstruction of PFC neural network activity based on repeated recordings difficult. First, no precise functional map, such as that found in sensory or motor cortices, has been established in the PFC except the eye movement direction map in the frontal eye field (Bruce et al., 1985). Second, PFC can be regarded as the highest order association cortex, and accordingly, its neural correlates are less clearly understood compared to those in sensory or motor cortices. Regarding working memory, neural dynamics during the delay period appear to be more complicated than simple reverberation for the maintenance of RM (Fuster, 1997; Miller, 1999). Third, discharges of PFC neurons are not independent but significantly correlated (Jung et al., 2000; Constantinidis and Goldman-Rakic, 2002). These characteristics limit significance of such analyses as reconstruction of population vectors based on successfully recorded unit activities (Georgopoulos et al., 1986). In this situation, functional interpretation of unit data would be greatly facilitated by monitoring activities of a large number of neurons simultaneously. Ensemble recording is advantageous in another respect; it permits obtaining a large amount of unit data. This facilitates investigation of neural dynamics in the course of learning a new task, which would be difficult with conventional recording techniques.

In the present study, we recorded from multiple single neurons in rat medial PFC (mPFC) in the course of learning a new delayed alternation task, in order to obtain insights into the dynamics of population code for working memory. Part of the present study has been presented previously in abstract form (Baeg et al., 2002, Soc. Neurosci., abstract 27, Program No. 677.19).

Results

Animal Behavior

Multiple single units were recorded from prelimbic and infralimbic cortices as rats (n = 5) were trained to alter-

*Correspondence: min@ajou.ac.kr

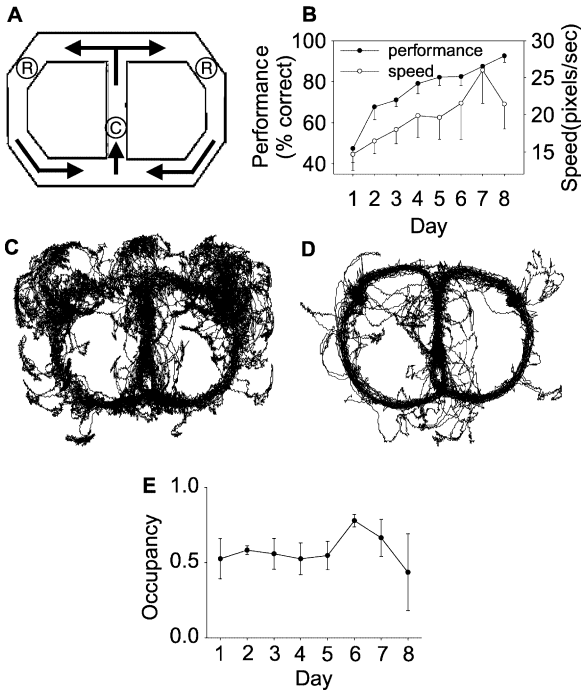

Figure 1. Animal Behavior

(A) Spatial delayed alternation task on a figure 8-shaped maze. The arrows indicate movement directions of the animal. Rats were rewarded on the two goal locations (®) and at the center (©) after a correct goal choice.

(B) Behavioral performance. The percentage of correct goal choice and the speed of the animal were enhanced as training progressed.

(C and D) Examples of movement trajectory on day 1 (C) and day 8 (D). The trajectory was divergent on the lower and upper ends on the central section of the maze depending on PG and FG, respectively. Only the portion of the central section that contained nondivergent trajectories was used as the delay period.

(E) PG-dependent divergence in movement trajectory in the course of training. The ordinate indicates pixel-by-pixel correlations between the left and right PG-associated occupancy distribution maps of the delay period.

nate two spatial locations to obtain a water reward on a figure 8-shaped maze (Figure 1A). The rats learned the task rapidly, improving from 47.5% ± 6.8% to 92.6% ± 3.2% correct choice over 8 days of training. Improvement was especially rapid across days 1 and 2. Also, as training progressed, the overall speed of the rat increased (Figure 1B), and the movement trajectory changed. Figure 1 shows two examples of cumulative animal trajectories in an early (day 1) and late (day 8) phase of training. As shown, the animal frequently made large lateral head movements on day 1 (Figure 1C). This behavior rapidly disappeared as training progressed (Figure 1D). In addition, as the rat exited the central section of the maze to approach either reward location, the animal trajectory diverged earlier (i.e., at a lower location) as training progressed.

The central section of the maze was meant to serve as the delay period. Because the lower and upper portions of the central section contained divergent trajectories depending on the previous goal choice (PG) and future goal choice (FG), respectively, we included in the delay period only the portion of the central section that contained nondivergent animal trajectories. Thus, the portion of the maze that corresponds to the delay period was different for each behavioral session. If the delay period was determined properly across different behavioral sessions, then the degree of PG- or FG-dependent trajectory divergence should be maintained similarly in the course of training. This was examined by calculating pixel-by-pixel correlations (pixel size: 0.18 × 0.18 cm) between the left and right PG-associated occupancy distribution maps of the delay period (data not shown for FG; similar results were obtained). As shown in Figure 1E, the levels of PG-dependent trajectory divergence were maintained similarly across the 8 days of training. A regression analysis indicated that the slope of the curve in Figure 1E was not significantly different from 0 ($p > 0.05$). Moreover, the animal spent the majority (84.8% ± 0.3%) of time during the delay period consuming water reward at an identical location (the central reward location), regardless of where the animal had come from (PG) or where it was going (FG). It is therefore unlikely that PG- or FG-dependent difference in the movement trajectory played a significant role in future goal choice behavior of the animals.

The length of delay was not significantly different depending on PG or FG in most sessions (unpaired Student's t test, $p > 0.05$; 31 out of 36 sessions for both PG and FG), and the velocity (calculated excluding the reward consumption period) of the animals during the delay period was not significantly different depending on PG or FG, either, in the majority of cases (unpaired Student's t test, $p > 0.05$; 25 and 23 out of 36 sessions for PG and FG, respectively). Moreover, the animals stopped completely at the beginning of the delay period to obtain water reward. Thus, there was no systematic difference in the length of delay or animal velocity depending on PG or FG. We were unable to detect any other type of behavior during the delay period that differed depending on PG or FG. The animal spent most of the delay duration consuming water reward at the central reward location across different trials; i.e., the animal behavior during the delay period was largely homogeneous regardless of PG or FG.

Neural Activity Changes during New Task Learning

We recorded from a total of 425 units from 5 rats. The units were recorded with variable stability (1–8 days of consecutive recordings), so that different unit populations were recorded in an overlapping manner across 8 days. Of all recorded units, we included in the analysis only those that emitted at least 100 spikes during the delay period across all trials. A total of 376 units (daily average of 10.4 ± 1.0 per rat, range of 2–25 units) were included in the analysis. The overall mean firing rate of the analyzed units was 7.2 ± 0.5 Hz. An example that shows changes in unit activity throughout 8 days of training is shown in Figure 2A. As shown, unit activity during the delay period increased in a manner dependent upon the goal choice as training progressed. Note that goal choice-dependent delay activity first appeared toward the end of training on day 1 and firing rate during the delay period increased over the first few days. Thirty-eight units (10.1% of all analyzed units) maintained continuously elevated activity throughout the delay period dependent upon PG as shown in Figure 2A (see below).

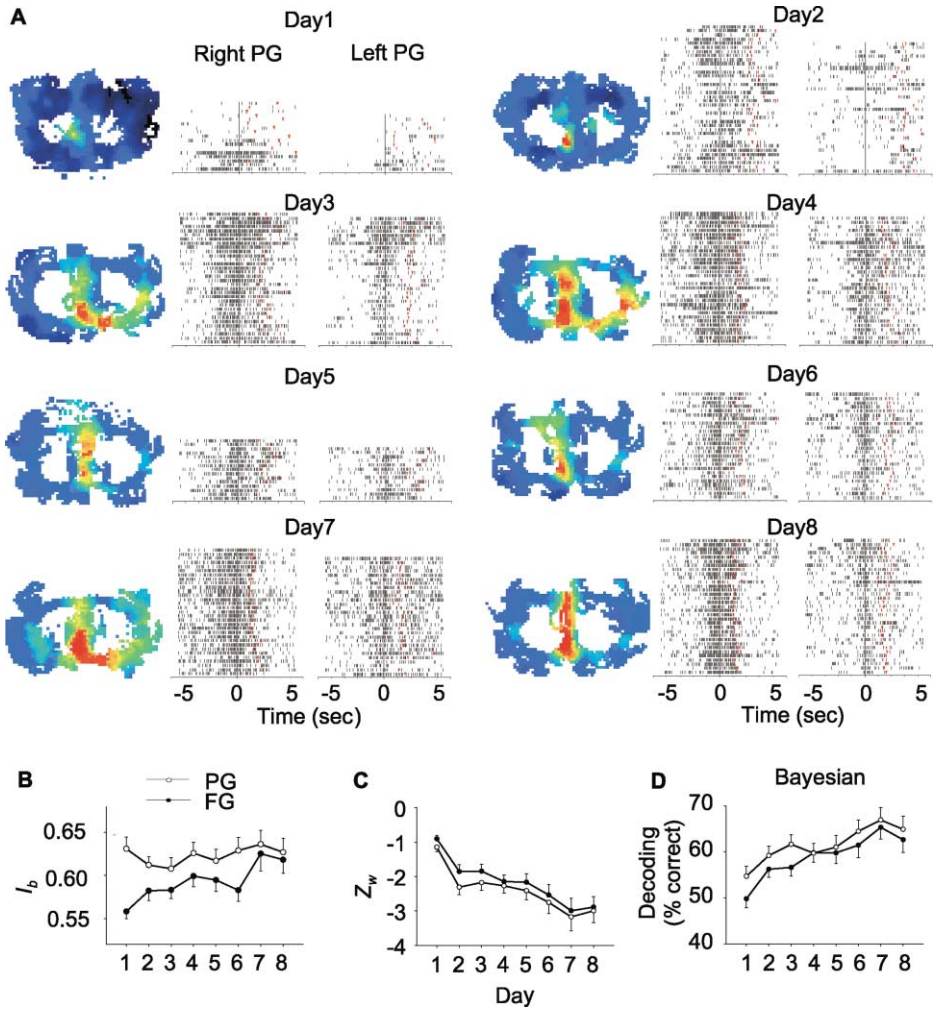

Figure 2. Changes in Single Neuron Activity during Learning

(A) Activity of a unit that was recorded for 8 consecutive days. Each spatial firing rate map shows the spatial distribution of the firing rate. Red indicates maximum firing rate (5 Hz). Two spike rasters in each day show unit activities during the delay period that were divided based on PG. Each line is a separate trial, and each tick mark indicates a spike. Trials were aligned relative to the beginning of delay period (time 0). The end of the delay period is indicated as red triangles on the right.

(B and C) Changes in I_b and Z_w are shown over the course of learning for PG and FG.

(D) Changes in the level of PG and FG decoding from single neuron activity.

Initially, we analyzed changes in single neuron activity during the delay period over the course of training. The index of biased firing (I_b) over 8 days of training showed different patterns of change for PG and FG. I_b for PG was relatively high as early as on day 1 and it increased only slowly, whereas I_b for FG was initially low, but increased rapidly over the course of training (Figure 2B). A regression analysis indicated that the slope of I_b curve for FG was significantly positive ($p < 0.001$) whereas that for PG was not significantly different from 0 ($p > 0.05$), indicating that PFC units showed substantial degrees of PG-dependent firing from the early phase of training. On the other hand, normalized rank sum value (Z_w) for both PG and FG changed so that unit firing was more biased depending on the goal choice as training progressed (Figure 2C). A regression analysis indicated that the slopes of both Z_w curves were significantly negative ($p < 0.001$ for both). These changes in I_b and Z_w suggest that mPFC neural activity conveyed greater amounts of information about PG and FG as the animals learned the task. This was examined by assessing how accurately PG or FG could be decoded from neuronal activity during the delay period. The Bayesian method showed improvement in decoding PG as well as FG over the time course of learning. A regression analysis indicated that the slopes of both decoding curves were significantly positive ($p < 0.001$ for both). The improvement reached 64.9% $\pm$ 2.9% and 62.6% $\pm$ 2.7% correct decoding of PG and FG, respectively, on day 8 ($n = 38$ units; Figure 2D), indicating that single mPFC neurons, on average, allow well-above chance prediction of PG and FG.

Next, we analyzed neuronal ensemble activities of the delay period in relation to behavior. Two different decoding methods, the template-matching and Bayesian methods, showed improvement in decoding PG as well

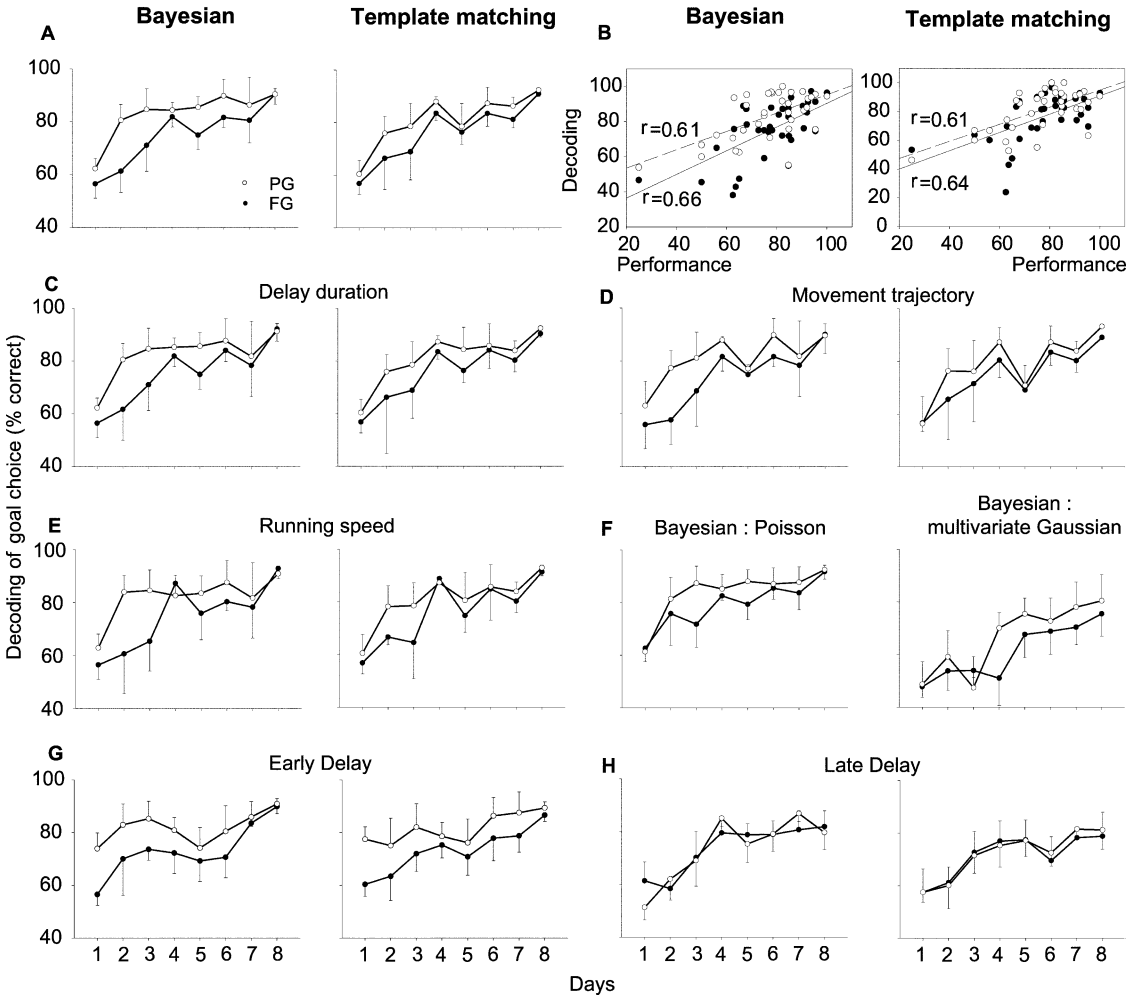

Figure 3. Changes in Neuronal Ensemble Activity during Learning

(A) Goal choice decoding based on neuronal ensemble activity of the entire delay period. Decoding results based on the Bayesian (left) and template-matching (right) protocols are shown for the previous (PG) and future goal choice (FG).

(B) Relationship between behavioral performance and goal choice decoding. The solid lines are results of a linear regression. Correlation coefficients (r) are indicated.

(C–E) Decoding was based on those sessions with similar delay durations across different goal choices (C), with correlation coefficients larger than 0.5 between left and right goal-associated occupancy distribution maps of the delay period (D), or with similar PG- or FG-dependent running velocity during the delay period (E).

(F) Goal choice decoding with the assumption of Poisson distribution (left) and multivariate Gaussian distribution (right) of unit activity. Note that the Bayesian method was used in both cases.

(G and H) Goal choice decoding based on the early and late delay period.

as FG from neuronal ensemble activity over the time course of learning (Figure 3A). A regression analysis indicated that the slopes of the goal choice decoding curves were significantly positive in all cases (Bayesian-PG, $p < 0.01$; Bayesian-FG, $p < 0.001$; template matching-PG, $p < 0.001$; template matching-FG, $p < 0.001$). The improvement in goal choice decoding was significantly and positively correlated with improvement in behavioral performance (i.e., percentage of correct goal choice; Figure 3B; $p < 0.01$ and $p < 0.001$ for PG and FG decoding with the Bayesian method, respectively; $p < 0.01$ and $p < 0.001$ for PG and FG decoding with the template-matching method, respectively).

In the following, we addressed the possibility that PG- or FG-dependent variations in animal behavior during the delay period, albeit small, can account for the improvement in goal choice decoding. We first examined the potential role of variations in the delay duration. We examined goal choice decoding based only on those sessions that had similar delay durations across different goal choices (31 out of 36 sessions for both PG and FG). As shown in Figure 3C, goal choice decoding was improved over the course of training, as in Figure 3A. The slopes of the goal choice decoding curves were significantly positive in all cases (regression analysis; Bayesian-PG, $p < 0.05$; Bayesian-FG, $p < 0.01$; template matching-PG, $p < 0.01$; template matching-FG, $p < 0.01$). Second, to examine the role of variations in the movement trajectory, we selected only those sessions with correlation coefficients between left and right goal-

associated occupancy distribution maps of the delay period larger than 0.5 (23 out of 36 sessions for both PG and FG). Again, goal choice decoding was similarly improved over the course of training. The slopes of the goal choice decoding curves were significantly positive in all but one case (Figure 3D; regression analysis; Bayesian-PG, $p > 0.05$; Bayesian-FG, $p < 0.05$; template matching-PG, $p < 0.01$; template matching-FG, $p < 0.05$). Moreover, no significant correlation was observed between the level of correlation in occupancy distribution and the level of PG or FG decoding (regardless of Bayesian or template-matching protocol; data not shown). Third, to examine the role of variations in running speed, we selected only those sessions with similar PG- or FG-dependent running velocity during the delay period (excluding reward consumption period) and examined goal choice decoding (25 and 23 out of 36 sessions for PG and FG, respectively). As shown in Figure 3E, goal choice decoding was similarly improved over the time course of training. The slopes of the goal choice decoding curves were significantly positive in all but one case (regression analysis; Bayesian-PG, $p > 0.05$; Bayesian-FG, $p < 0.05$; template matching-PG, $p < 0.05$; template matching-FG, $p < 0.001$). No significant improvement in PG decoding (the Bayesian method) is probably attributable to neural activity in the early delay period that conveyed a substantial amount of information about PG in the early phase of training (see below). Combined, these analysis results further corroborate the possibility that goal choice decoding improved as training progressed not because of time-dependent changes in animal behavior but because of changes in neural activity that conveyed progressively more information about PG and FG.

In order to compare our results with the previous studies that employed different assumptions about the probability of unit discharge, we examined goal choice decoding based on spike count data with the assumption that each spike train is an independent Poisson process (Zhang et al., 1998). For this, we did not normalize spike counts relative to the length of delay. Instead, we only included those sessions (31 out of 36 for both PG and FG) in which delay durations were similar between left versus right goal-associated trials. Goal choice decoding was improved over the course of training (Figure 3F, left) as was the case of firing rate-based decoding (using Gaussian distribution), shown in Figure 3A. The slopes of both goal choice decoding curves were significantly positive (regression analysis; PG, $p < 0.01$; FG, $p < 0.001$). The maximum levels of decoding on day 8 were similar to those shown in Figure 3A (PG, 90.4% $\pm$ 2.3% and 92.4% $\pm$ 1.8% for Gaussian and Poisson distribution, respectively; independent samples Student's t test, $p > 0.05$; FG, 90.4% $\pm$ 3.7% and 91.7% $\pm$ 2.6% for Gaussian and Poisson distribution, respectively; independent-samples Student's t test, $p > 0.05$). In pilot studies, we explored multivariate Gaussian distribution of unit firing, which takes neuronal interactions into account (Oram et al., 1998). As shown in Figure 3F, the level of goal choice decoding improved over training days. The slopes of both goal choice decoding curves were significantly positive (regression analysis; PG, $p < 0.01$; FG, $p < 0.01$). The maximum levels of decoding (80.5% $\pm$ 9.9% and 75.5% $\pm$ 8.5% for PG and FG, respectively, on day 8) were not significantly different from those shown in Figure 3A (independent samples Student's t test, $p > 0.05$ for both PG and FG comparisons). The use of the multivariate Gaussian distribution did not improve goal choice decoding from neuronal ensemble activities in 1 s time windows either (data not shown). Furthermore, goal choice decoding with multivariate Gaussian distribution, after destroying temporal relationships among simultaneously recorded units by random shuffling of trials, yielded similar levels of decoding, as shown in Figure 3F (data not shown). Thus, correlated neuronal discharges did not contribute much to goal choice decoding at the time scale >1 s. We therefore employed the assumption of independent Gaussian distribution of unit activity in the subsequent decoding analyses.

Because previous studies in monkey PFC suggest temporally distinct representations of RM and PM within the delay period (Rainer et al., 1999; Takeda and Funahashi, 2002), we separately analyzed neuronal ensemble data from the initial and last 1 s of the delay period. After excluding those units that emitted less than 100 spikes during the selected time periods of the delay across all trials, 252 and 254 neurons (daily average: 7.2 $\pm$ 0.4 and 7.3 $\pm$ 0.5 per rat) were included in the analyses for the early and late delay period, respectively. The overall mean firing rates of the analyzed units were 9.8 $\pm$ 0.5 and 13.0 $\pm$ 0.7 Hz, respectively. Neuronal ensemble activity in the early delay period allowed a relatively high level (75% correct) of PG decoding even on day 1, and it increased only slowly over the course of learning. On the other hand, decoding of FG was closer to chance level on day 1 and increased more rapidly (Figure 3G). A regression analysis indicated that the slopes of the FG decoding curves were significantly positive (Bayesian: $p < 0.01$; template matching: $p < 0.01$) but those of the PG decoding curves were not significantly different from 0 ($p > 0.05$). Also, significant differences between PG and FG decoding were observed on day 1 for both the template and Bayesian methods (paired Student's t test, $p < 0.05$ for both). Regarding the late delay period (Figure 3H), the slopes of the goal choice decoding curves were significantly positive in all cases (Bayesian-PG, $p < 0.001$; Bayesian-FG, $p < 0.001$; template matching-PG, $p < 0.01$; template matching-FG, $p < 0.05$). No significant difference was observed between PG and FG decoding on day 1 for the late or entire delay period (paired Student's t test, $p > 0.05$ for all measures). These results indicate that information about PG (i.e., RM) existed in the early delay period even on day 1 but that information was not maintained across the entire delay period. As learning progressed, however, neuronal ensemble activity across the entire delay period increasingly conveyed information about both PG and FG.

Comparison between Correct and Error Trials

It is difficult to distinguish whether neural activity during the delay period represents RM of PG or PM for FG in well-trained rats because the information about PG allows decoding of FG and vice versa as behavioral performance improves. This problem is avoided if we select only error trials (consecutive visits to the same

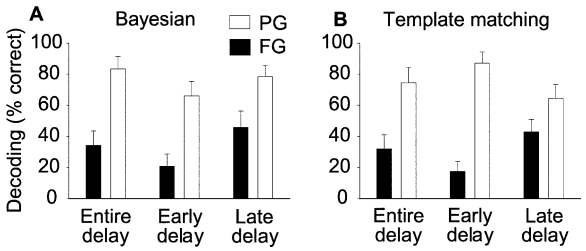

Figure 4. Neuronal Ensemble Activities in Error Trials Allow Decoding of PG

(A and B) Decoding of PG and FG from neuronal ensemble activity during the early, late, and entire delay period in error trials are shown for the late (days 5–8) phase of training.

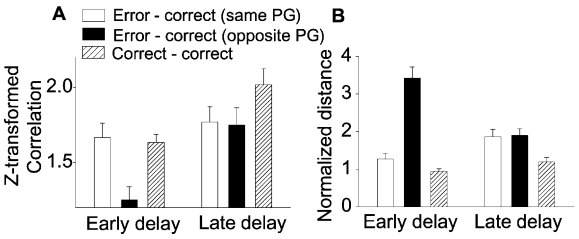

Figure 5. Comparison between Correct and Error Trials

(A) Correlations of neuronal ensemble activity among correct and error trials with the same or opposite PG.

(B) Normalized distances of neuronal ensemble activity across correct and error trials with the same or opposite PG.

goal) in the test phase (training phase consists of mostly correct trials). Because the animals committed fewer errors as training progressed, we combined the data between days 5 and 8 (comprising 86% correct and 14% error trials). Possible expected outcomes are decoding of PG (RM), FG (PM), or neither (RM-PM association or failure to maintain either). Neuronal ensemble activity in the early, late, and entire delay period allowed better decoding of PG compared to decoding of FG (paired Student's t test, $p < 0.05$ for all comparisons; $n = 17$ sessions, 4.2 average errors per session; Figures 4A and 4B). Because the firing rate templates were constructed based on mostly correct trials (86%) in well-trained animals, the levels of correct decoding of PG and FG based on error trials tended to be opposite. These results show that neural activity across the entire delay period in error trials carried information about PG (RM) after enough training, indicating that the animals did not commit errors because of simple forgetting of PG during the delay period. Consistent with this possibility, neural activity was similar between error and correct trials during the initial (10.2 ± 0.4 versus 9.8 ± 0.4 Hz, paired Student's t test, $p > 0.05$) as well as the last 1 s of the delay period (13.2 ± 0.6 versus 13.0 ± 0.5 Hz, paired Student's t test, $p > 0.05$).

To obtain insights into the nature of information conveyed in correct trials, we compared neuronal activity between correct and error trials in the early and late delay period. All trials were divided into four groups, depending on the combination of PG and FG (LR, LL, RL, and RR). Then, as many correct trials (LR and RL) as the number of error trials (LL and RR, respectively) were randomly selected, and correlations were measured between the selected and remaining correct trials (correct-correct correlation; LR versus LR and RL versus RL), between error trials and the remaining correct trials with the same PG (error-correct correlation with the same PG; RR versus RL and LL versus LR), and between error trials and the remaining correct trials with the opposite PG (error-correct correlation with the opposite PG; RR versus LR and LL versus RL). All correlation coefficients were converted to Fisher's *z* for normalization in this analysis (Rosner, 1995). We also measured normalized Euclidian distances in neuronal ensemble activities among these groups, using a discriminant analysis. If a given portion of the delay period (e.g., the early delay period) carried information about PG (RM) as in error trials, then neural activities in correct trials would be similar to those in error trials with the same PG. Consequently, correct-correct correlation (distance) would be similar to error-correct correlation (distance) with the same PG. Otherwise, i.e., a different type of information than RM was processed in correct trials, then neural activities in correct trials would be less similar to those in error trials. In this case, correct-correct correlation (distance) would be greater (shorter) than error-correct correlations (distances). As shown in Figure 5A, correct-correct correlation was similar to error-correct correlation with the same PG but significantly higher than error-correct correlation with the opposite PG in the early delay period (one-way ANOVA, $p < 0.001$; post hoc Scheffe test, correct-correct correlation versus error-correct correlation with the opposite PG, $p < 0.001$; error-correct correlation with the same PG versus error-correct correlation with the opposite PG, $p < 0.001$). Similarly, correct-correct distance was similar to error-correct distance with the same PG but significantly shorter than error-correct distance with the opposite PG (one-way ANOVA, $p < 0.001$; post hoc Scheffe test, correct-correct distance versus error-correct distance with the opposite PG, $p < 0.01$; error-correct distance with the same PG versus error-correct distance with the opposite PG, $p < 0.01$; Figure 5B), suggesting that similar information (PG) was processed across error and correct trials in the early delay period. In the late delay period, correct-correct correlation was higher than error-correct correlations, but this difference was not statistically significant (one-way ANOVA, $p > 0.05$; Figure 5A). However, correct-correct distance was significantly shorter than both types of error-correct distance (one-way ANOVA, $p < 0.001$; post hoc Scheffe test, correct-correct distance versus error-correct distance with the same PG, $p < 0.001$; correct-correct distance versus error-correct distance with the opposite PG, $p < 0.001$; Figure 5B). These results show that neuronal activities are similar between error and correct trials with the same PG in the early delay period but somewhat different between error and correct trials in the late delay period.

Size of Neural Population

To assess the relationship between the number of units in the ensemble and the level of correct goal decoding, the number of units was systematically reduced. We used the data from days 5–8 for this analysis. For each

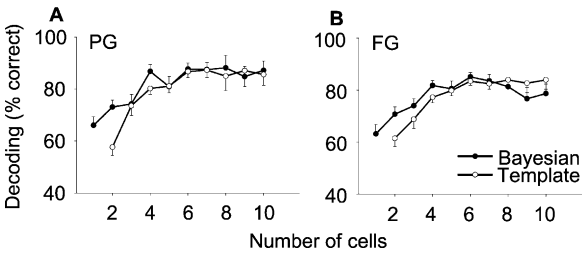

Figure 6. Cell Number and Goal Choice Decoding

(A and B) The relationship between the number of cells and neuronal ensemble-based decoding of PG or FG in well-trained rats (days 5–8).

step of cell number reduction, the corresponding number of cells was randomly selected for omission. Correct decoding (based on the entire delay period) of PG and FG reached near maximal level (80%) with only four or five neurons on average (Figures 6A and 6B). These results demonstrate that a small subset of mPFC neurons conveyed a large amount of information about PG and FG.

Decoding without Continuous Delay Cells

A number of units exhibited different levels of activity depending on PG or FG during the delay period in well-trained rats (differential delay cells, DDCs). Some of the differential neurons maintained PG-specific activities throughout the entire delay period (continuous DDCs, Figure 7A). Thirty-eight of 376 neurons (10.1%) were determined to be continuous DDCs. Other neurons maintained PG-specific activities only during a certain part of the delay period (noncontinuous DDCs, Figure 7B). Eighty neurons (21.3%) fell into this category. Although the role of continuous delay cells in working memory has been emphasized (see Introduction), a population of noncontinuous DDCs may mediate working memory as well, based on sequential activation ("relay race") (Batuev et al., 1980). We investigated this possibility by testing PG decoding excluding continuous DDCs. We only show here PG decoding results, but similar results were obtained with the analyses concerning FG decoding (data not shown). Because average duration of the delay was short (3.2 ± 0.2 s) on day 8, we chose day 5 data for this analysis (average delay duration: 5.1 ± 0.3 s). Decoding was based on neuronal ensemble activity within a 1 s time window that moved at 50 ms time steps. Because the average delay duration was $\sim$5 s, we moved the window up to 1.5 s forward from the beginning, and up to 1.5 s backward from the end of the delay period. Figures 7C and 7D shows PG decoding with and without continuous DDCs in these time windows. As shown, neuronal ensemble activity without continuous DDCs (10% of day 5 unit data) allowed significant decoding of PG across the entire delay period. The level of correct decoding was reduced as the 1 s time window moved toward the middle of the delay period. This is because of variable delay durations across different trials and dependence of unit discharge upon position on the maze rather than time of delay (Figure 8, see below). Also, because the delay duration was shorter than 2.5 s in some trials, decoding toward the middle of the delay period was contaminated by neural activities outside the delay period. Nevertheless, the level of goal choice decoding was similar with and without continuous DDCs at most time steps. This is because activities of noncontinuous DDCs were distributed throughout the delay period so that each time window contained some of them. Figure 7E shows an example of simultaneously recorded unit responses during the delay period, excluding continuous DDCs.

The above result could be contaminated from continuous DDCs that were spuriously classified as noncontinuous DDCs according to our criteria. To avoid such possibility, we visually examined all noncontinuous DDCs recorded on day 5. No case of subjectively apparent "continuous DDC" was detected. We also changed the definition of continuous DDCs so that more units were classified as continuous DDCs (see Experimental Procedures) and excluded newly defined continuous DDCs (20% of day 5 unit data) from the neural population. Results from goal choice decoding with a moving box of 1 s time window are shown in Figures 7F and 7G. As shown, neuronal ensemble activity without newly defined continuous DDCs allowed significant decoding of PG across the entire delay period, albeit at lower levels than control at some time steps with the template-matching protocol. These results indicate that the maintenance of working memory by a group of noncontinuous DDCs is not because of spurious classification of continuous DDCs as noncontinuous DDCs.

Temporal and Positional Reliability of Unit Discharge

In order to determine whether unit activities are associated with time of delay or position on the maze, we compared variations of neural activity in the temporal and spatial domains. Because we were interested in temporal and positional variations of spike trains across trials, rather than those of individual spikes within a spike train, the time and position of a spike train (mean spike time and position of all spikes in the delay period) relative to the beginning of delay were first determined for each trial and then SDs of time and positions of spike trains across all trials were computed. For comparison, the time and positions of spikes were normalized relative to the mean duration and distance of the delay period of a given session. Figure 8 shows temporal and positional variations of the delay period spike trains of all neurons. Most points were found below the 45° line (toward the temporal domain), indicating that the variation in the temporal domain tended to be higher than in the spatial domain. The average SDs of time and position were 0.58 ± 0.54 and 0.20 ± 0.09 ($n = 376$), respectively, which were significantly different (paired Student's t test, $p < 0.001$). These results indicate that the position on the maze is a more important factor than the time of delay for mPFC unit discharge in the current task.

Discussion

Development of Neural Representations for Working Memory

Learning is an essential component of PFC functions. In order for an animal to survive in an ever-changing

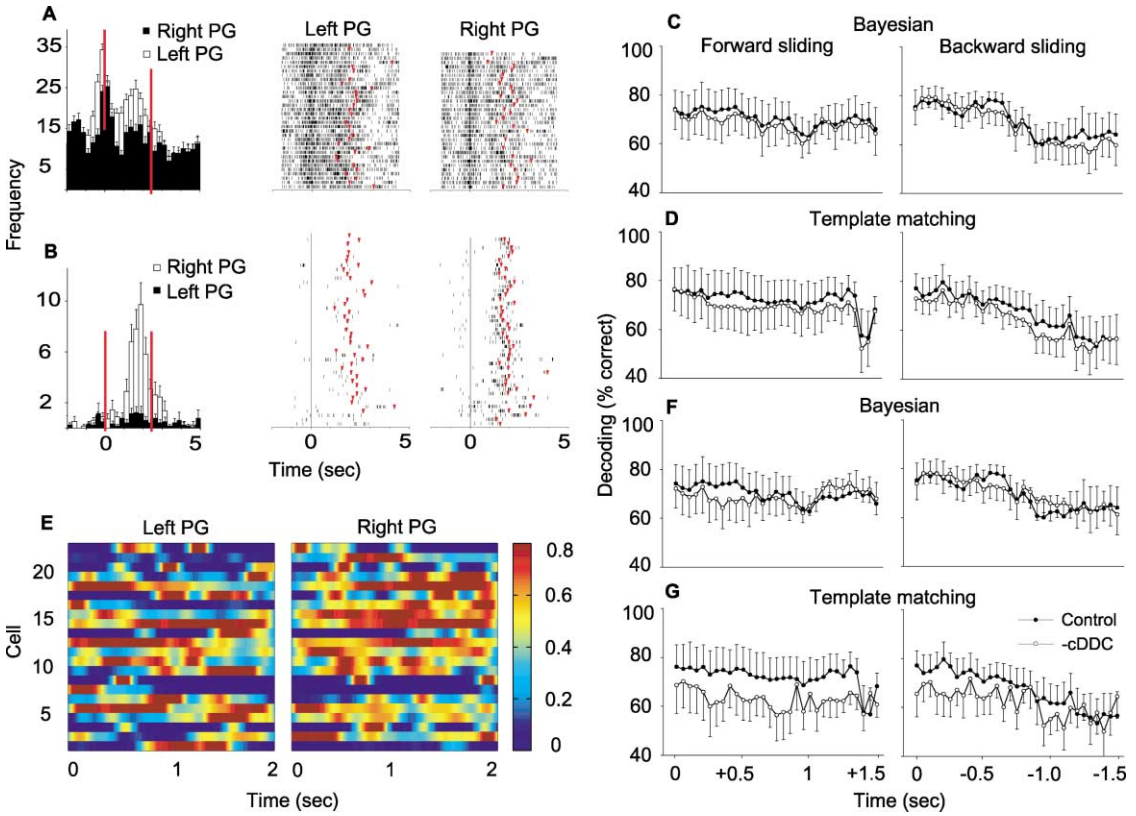

Figure 7. Goal-Choice Decoding without Continuous DDCs

(A) A continuous DDC. This unit elevated its firing rate throughout the delay period after the left PG. Red vertical lines on the perievent time histogram denote the beginning and the average end of the delay period. Spike rasters were constructed as in Figure 2.

(B) A noncontinuous DDC. This unit elevated its firing rate toward the end of the delay period after the right PG.

(C and D) Levels of PG decoding from neuronal ensemble activities with and without continuous DDCs are compared. Decoding was based on a 1 s time window of neuronal ensemble activity that moved forward (indicated as "+" on the abscissa) in 50 ms steps from the beginning of the delay period (time 0; left) or backward ("−" on the abscissa) from the end of the delay period (time 0; right). −cDDC, decoding without continuous DDCs.

(E) This example shows activities of simultaneously recorded PFC units that were divided based on PG, excluding continuous DDCs. Neurons other than DDCs and noncontinuous DDCs are shown together. The abscissa and ordinate indicate time (time 0 denoting beginning of the delay period) and unit number, respectively. Firing rates were calculated in 10 ms time bins and were smoothed using a Gaussian window function with δ_t = 100 ms. Colors indicate firing rates that were normalized relative to the maximum firing rate of each neuron (minimum 1 Hz). Firing rates 80% or higher of the maximum firing rate are indicated in the same color (red). As shown, different noncontinuous DDCs elevated firing rates in different parts of the delay period so that the unit population conveyed information about the PG across the entire delay period.

(F and G) Levels of PG decoding from neuronal ensemble activities with and without more broadly defined continuous DDCs are compared. Conventions are as in (C) and (D).

environment, it has to adaptively modify its behavior according to environmental changes. As the PFC subserves planning of future behavior (Fuster, 1997), the PFC must adjust its activity according to changes in environment so that the most appropriate behaviors are generated in a given situation. In this regard, one of the well-known deficits that occurs following damage in the PFC is the inability of the animal to adapt to changes in behavioral tasks (Fuster, 1997), and activities of PFC neurons are rapidly modified during learning (e.g., Rainer and Miller, 2000; Baeg et al., 2001). We can expect from these studies that PFC population code for working memory will change dynamically as the animal learns a new working memory task. By using the multiple single neuron recording technique in the present study, we were able to record a large number of neurons at the same time and keep track of neural activity change over the course of learning a new delayed alternation task. The results show that neuronal ensemble activities during the delay period conveyed increasing amounts of information about PG and FG as training progressed, indicating that representations of working memory develop in the PFC in parallel with behavioral learning. In well-trained rats, less than 30 neurons allowed ~90% correct decoding of PG and FG. A previous study has shown that discrimination of future lever choice is possible based on activities of ~10 simultaneously recorded rat mPFC neurons during 1 s period prior to the lever press behavior (Chang et al., 2000). One surprising result of the present study was that only a few neurons (four to five) permitted the near maximal level of goal choice decoding. At the single cell level, a PFC neuron allowed better than 60% correct decoding of goal choice on average. These results indicate that, after learning,

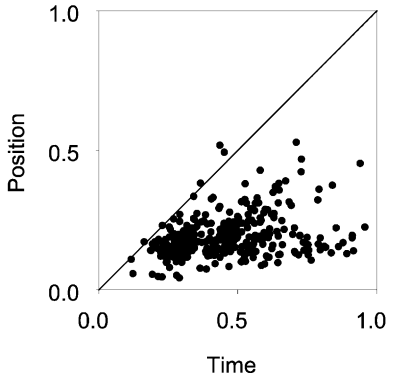

Figure 8. Temporal and Positional Reliability of Unit Discharge

The scatter plot shows the distribution of temporal and positional variations of all analyzed units (n = 376). Each point represents SDs of time (abscissa) and position (ordinate) of spike trains since the beginning of delay across all trials for one neuron. Points below (above) 45° line indicate larger (smaller) temporal than positional variation. Not shown in this plot are 21 points that had temporal or positional SD values larger than 1.0.

working memory is robustly and redundantly represented among PFC neurons.

The present results suggest that the PFC "learned" to maintain initially available working memory throughout the entire delay period. Decoding of PG was possible even on day 1 in the early delay period, and, as training progressed, correct decoding of PG and FG was possible across the entire delay period, indicating that initially available information about PG in the early delay period became available throughout the entire delay period. What is the neural mechanism underlying the observed changes in neural activity? The animals were rewarded only after correct behavioral choices (alternation) in the present study (reinforcement learning; Sutton and Barto, 1998). It is possible that, when a correct choice is made, the past sequence of neural activity gets reinforced so that neural activity in the late delay period is associated with that in the early delay period. This will lead to a gradual development of delay period neural activity that differentiates left versus right PG (and FG). This possibility is consistent with the "relay race" hypothesis of working memory maintenance across the delay period (Batuev et al., 1980). Alternatively, the animals may have captured the "rule" of the task in an abrupt manner (especially between days 1 and 2). In any case, considering that long-term potentiation and long-term depression have been demonstrated in rat mPFC (Laroche et al., 1990; Hirsch and Crepel, 1990; Herry et al., 1999; Gemmell and O'Mara, 2000; Kim et al., 2003), it is likely that synaptic weight changes within the mPFC are at least partly responsible for the observed changes in neural activity.

Conversion of Retrospective Memory into Prospective Memory

Some delay cells recorded in monkey PFC slowly decrease their activities, whereas others slowly increase their activities during the delay period (Fuster, 1997). In a task that allowed dissociation of neural correlates between sensory cues and behavioral choices, some PFC neurons respond to specific sensory cues and some to behavioral responses, suggesting that both RM and PM are represented in the PFC (Niki and Watanabe, 1976; Quintana and Fuster, 1992; Funahashi et al., 1993). The present study shows that neuronal activities carried information about PG (RM) across the entire delay period in error trials after enough training (Figure 4). It is therefore unlikely that the animals committed errors because of simple forgetting of PG (i.e., failure to maintain RM) during the delay period. Further analyses indicated that neuronal activities were similar between error and correct trials that shared the same PG in the early delay period, suggesting that information about PG (RM) was conveyed in this period of correct trials. Because the current template-matching method was based on comparing correlation coefficients, similar correct-correct correlation with error-correct correlation with the same PG (Figure 5A) indicates that correct and error trials are not different in decoding PG in the early delay period as long as the template-matching method is concerned.

On the other hand, neuronal activities were different between correct and error trials in the late delay period. It is possible that neuronal ensemble activity in the late delay period of correct trials conveyed information about PG more faithfully than that in error trials, and behavioral errors are attributable to insufficient maintenance of RM in the late delay period in error trials. This is not very likely, because considerable decoding of PG was possible from activities of less than 30 neurons in the late delay period of error trials. If the entire mPFC is concerned, the RM of PG would be much more faithfully represented. These considerations lead to an alternative possibility that RM was successfully transformed to PM across the delay period in correct trials but not in error trials, so that neural activity in the late delay period of of correct trials largely conveyed information about FG. This possibility is consistent with previous studies that suggested transformation from retrospective to prospective coding across the delay period in monkey PFC (Rainer et al., 1999; Takeda and Funahashi, 2002). The present results do not provide direct evidence for this possibility, however, because of the nature of the behavioral task employed (delayed alternation). Future work employing an appropriately designed behavioral task is needed to obtain more direct evidence.

Maintenance of Working Memory

The precise neural mechanisms underlying maintenance of working memory are not clear. Sustained neuronal activity throughout the delay period based on synaptic reverberation in a recurrent circuit has been proposed as one possible mechanism (see Wang, 2001, for review). Recently, neurons in the entorhinal cortex were found to sustain multiple levels of firing rates depending on input strengths without interactions with other neurons (Egorov et al., 2002), raising the possibility that working memory is maintained by single cell-based regenerative activities. On the other hand, Batuev et al. (1980) have proposed that working memory is mediated by sequential activation of different neural populations (relay race). In this case, each neuron does not have to maintain continuous neural activity throughout the delay period. This type of neurons has been found in monkey PFC

(Batuev et al., 1979) and in the present study (noncontinuous DDCs). When we excluded continuous DDCs, the remaining neurons conveyed information about PG and FG across the entire delay period, indicating that working memory can be mediated by sequential activation of different neural populations. Continuous DDCs, which comprise ~10% of the analyzed units, may merely act as "summators" of noncontinuous DDC activities (Batuev et al., 1980). On the other hand, it is possible that continuous DDCs convey information independently from noncontinuous DDCs. Multiple mechanisms may operate in parallel in the PFC for the maintenance of working memory. Additional work is needed to clarify this matter.

Regarding factors that determine discharges of noncontinuous DDCs, the duration of the delay period varied from trial to trial in the present study. It is therefore unlikely that a group of neurons (i.e., noncontinuous DDCs) was sequentially activated with fixed time delays. Rather, it is more likely that activity of a neuron was associated with a location on the maze (Jung et al., 1998). Indeed, activities of PFC units during the delay period were more consistent in the spatial than the temporal domain (Figure 8). If neuronal activity is associated with a spatial location as well as previously active neurons, its response could be similar to those of noncontinuous DDCs. If we assume that an animal moves to a location on the maze that corresponds to the beginning of the delay period, then some noncontinuous DDCs (population A) may elevate their activities at this location that are differential depending upon discharges of a particular set of neurons at the previous location (i.e., depending on PG). They may maintain their activities there by synaptic reverberation (Wang, 2001) or single cell-based activity regeneration (Egorov et al., 2002). As the animal moves to a new location, a different set of noncontinuous DDCs (population B) may elevate their activities that are differential depending upon the activities of population A, and neurons in population A cease firing at the new location. Again, neurons in population B maintain their activities by synaptic reverberation or single cell-based activity regeneration. This process may continue all the way across the delay period. In other words, persistent neuronal activity over a short time scale operates in parallel with sequential activation of different neural populations over a longer time scale for the maintenance of working memory (Batuev et al., 1980), and spatial information provides a signal for activity transition among different neural populations. Future work is needed to determine whether the mPFC indeed maintains working memory in this manner in the current task.

Experimental Procedures

Behavioral Task

The behavioral task was a spatial delayed alternation task on a figure 8-shaped maze (Jung et al., 1998). The dimension of the maze was 90 × 50 cm, and the width of the track was 9–13 cm. It was elevated from the floor with 40 cm high walls along the entire track. Five male Sprague-Dawley rats (9–13 weeks old) were trained to alternate between two spatial locations (®, Figure 1A) on the maze to obtain water reward for 8 days. They were required to go through the central section of the maze, regardless of PG. Thus, the central section of the maze served as the delay period during which RM of PG or PM for FG should be maintained. Rats were rewarded at the center (©, Figure 1A) after a correct goal choice. Only the portion of the central section that contained nondivergent trajectories was used as the delay period. The duration of the delay period was 5.1 ± 0.2 s, and it decreased as learning progressed (9.4 ± 0.9 s on day 1 and 3.2 ± 0.3 s on day 8). Rats were trained over 29.0 ± 1.6 complete trials (one complete trial consists of visiting both goals) per day. The experimental protocol was approved by the Ethics Review Committee for Animal Experimentation of Ajou University.

Unit Recording

A microdrive array (Neuro-hyperdrive, Kopf Instruments, Tujunga, CA) was loaded with 12 tetrodes and implanted in the left or right mPFC (2.7 mm A, 0.7 mm L from bregma) under deep anesthesia with sodium pentobarbital (50 mg/kg body weight). Tetrodes (Recce and O'Keefe, 1989, Soc. Neurosci., abstract; Wilson and McNaughton, 1993) were fabricated by twisting four strands of polyimide-insulated nichrome wires (H.P. Reid Co., Palm Coast, FL) together and gently heated to fuse the insulation without short-circuiting the wires (final overall diameter, 40 μm). The electrode tips were cut and gold plated to reduce impedance to 0.3–0.6 MΩ measured at 1 kHz. Following 7–10 days of recovery from surgery, tetrodes were gradually advanced to obtain unit signals. When multiple well-isolated unit signals were obtained, unit recording and behavioral training began simultaneously (day 1). Unit signals via a headstage of complementary metal oxide semiconductor (CMOS) operational amplifier (Neuralynx, Tucson, AZ) were amplified 5000–10,000×, filtered between 0.6 and 6 kHz, digitized at 32 kHz, and stored on a SUN4u workstation using the Cheetah data acquisition system (Neuralynx). The head position of the animal was also recorded at 60 Hz by tracking an array of light-emitting diodes mounted on the headstage. When recordings were completed, small marker lesions were made, and recording locations were verified histologically.

Analysis

Isolation of Single Units

Single units were isolated by projecting the four channel relative amplitude data two dimensionally and manually applying boundaries to each subjectively apparent unit cluster using custom software (Xclust, M. Wilson). Spike width was also used as an additional spike waveform characteristic for unit isolation. To prevent potential overlap of unit signals, only those pairs of unit clusters that were completely nonoverlapping in at least one of the two-dimensional projections of spike amplitude data were included in the analysis.

Index of Biased Firing

The index of biased firing (I_b) was calculated as follows:

$$I_b = \max f(g)/\sum f(g),$$

where *f(g)* denotes mean firing rate during the delay period associated with either (left or right) goal choice *(g)*. The function max finds the value of g that maximizes the argument. The possible range of I_b is between 0.5 and 1. As neural activity conveys more information about PG or FG, the firing rate of a neuron during the delay period would be more biased toward either goal choice (I_b approaches 1).

Normalized Rank Sum Value

I_b measures the overall firing rate bias between two goal choices averaged across all trials. To assess trial-to-trial variations in relative strengths of unit activity (i.e., firing rates) associated with either goal choice, we calculated normalized rank sum value (Z_w). The procedure of obtaining Z_w is part of Wilcoxon rank sum test (Rosner, 1995).

Decoding of Goal Choice

The template-matching and Bayesian methods were used as described previously (Zhang et al., 1998; Oram et al., 1998). The data from the trials of a given day were divided into two halves, so that the first and second halves served as the training and test phases, respectively. Then the average firing rates of all neurons in the training phase were obtained for each goal choice:

$$\mathbf{f}(g) = (f_1(g), f_2(g), \ldots, f_N(g)),$$

where g denotes goal choice (either left or right). Decoding of goal choice was based on a firing rate vector of each trial in the test phase:

$$\mathbf{r} = (r_1, r_2, \ldots, r_N).$$

Various scaling methods can be used for the template-matching method. We used the following method, which is equivalent to comparing Pearson's correlation coefficients, because it yielded the best performance among various scaling methods we tested:

$$\text{Decoded goal choice} = \max \frac{\sum(r_i - \bar{r})(f_i(g) - \overline{f(g)})}{\sqrt{\sum(r_i - \bar{r})^2 \sum(f_i(g) - \overline{f(g)})^2}}$$

where $\overline{f(g)}$ and $\bar{r}$ indicate the mean firing rates averaged over N neurons during training and test phases, respectively.

Bayesian or probabilistic decoding was performed as follows:

$$\text{Decoded goal choice} = \max P(g|\mathbf{r}).$$

$P(g|\mathbf{r})$ was calculated from the following formula of conditional probability:

$$P(g|\mathbf{r})P(\mathbf{r}) = P(\mathbf{r}|g)P(g),$$

where $P(g)$ is the probability of goal choice by the animal and $P(\mathbf{r}|g)$ is the probability for the firing rate vector $\mathbf{r}$ to occur that is associated with either goal choice. The probability $P(\mathbf{r})$ for the firing rate vector $\mathbf{r}$ was not calculated because it was common for both goal choices. $P(\mathbf{r}|g)$ was calculated as the following assuming Gaussian distribution of unit activity data:

$$P(\mathbf{r}|g) = \prod_{i=1}^{N} \frac{1}{\sigma_i\sqrt{2\pi}} e^{-\frac{1}{2}(r_i - \mu_i)^2/\sigma_i^2}$$

for each g, where μ_i and σ_i denote mean and SD of activity of neuron i, respectively, that were calculated from unit activity data during the training phase [μ_i is equivalent to $f_i(g)$].

Correlation between Error and Correct Trials

All trials in a given session were divided into four groups depending on the combination of previous and future goal choices as follows: left-right (LR), right-left (RL), left-left (LL), and right-right (RR) goal choices. We then divided each type of correct trial (LR and RL) into two subgroups. One group contained as many trials as the numbers of corresponding error trials (LR and RL as many as LL and RR, respectively), and the other group contained the remaining correct trials. Firing rate profiles of the remaining correct trials in a given session were averaged to obtain a single firing rate profile. Pearson's correlation coefficient was calculated between averaged firing rates of the remaining correct trials and firing rates of each of error trials and selected correct trials and then transformed to Fisher's z for normalization (Rosner, 1995). Correlations were calculated between the selected and remaining correct trials (LR versus LR and RL versus RL), between error trials and the remaining correct trials with the same PG (LL versus LR and RR versus RL), and between error trials and the remaining correct trials with the opposite PG (LL versus RL and RR versus LR). This procedure was repeated for all error trials and the selected correct trials (n = 71 each) and correlation coefficients, following Fisher's z transformation, were averaged according to the corresponding comparisons.

Discriminate Function

Neuronal ensemble activities between correct and error trials were also compared using a discriminate function. One-dimensional discriminate function was generated based on neuronal ensemble activities in the remaining correct trials. The coefficient was computed so that the linear combinations of firing rates maximized the ratio of differences between two group means (LR versus RL; discrimination analysis of SPSS, version 10). In discrimination analysis, discriminate functions are used to determine to which group (LR versus RL) new data belong. Our purpose was to measure relative distance (i.e., relative difference in firing rate profile) between neuronal ensemble activities of the remaining correct trials and error trials (or selected correct trials). Thus, instead of classifying error trials and selected correct trials as LR or RL, we computed normalized distances between discriminate variables of the remaining correct trials and error trials (or selected correct trials). For this, means and SDs of discriminate variables of LR and RL of the remaining correct trials were calculated for each session, and distances between each error trial (or selected correct trial) and means of LR and RL of the remaining correct trials were expressed as SDs of the corresponding remaining correct trials. Distances were averaged according to the same PG (LL-LR and RR-RL) or opposite PG (LL-RL and RR-LR).

Differential Delay Cells

We first determined the units that showed differential firing in the delay period depending on PG. Firing rates during the delay period of all trials were divided into two groups according to PG, and they were compared with a Student's t test. Those units with p values <0.01 were determined to be DDCs. Continuous DDCs were further selected from the DDCs with the following. Those trials that were associated with preferential PG were selected and then each delay period of the selected trials was divided into four equal durations, and average firing rate was calculated for each duration across all trials. If average firing rates of all four durations were higher than the average firing rate during the time periods on the maze other than the delay, the unit was considered as continuous DDCs. The rest were determined to be noncontinuous DDCs. When examining the role of noncontinuous DDCs in maintaining working memory, continuous DDCs were sometimes more broadly defined to exclude more units from the population. In such cases, those DDCs with average firing rates of at least three delay durations (instead of four) exceeding the average firing rate in the other periods of time except the delay periods were defined as continuous DDCs.

Statistical Tests

All data are expressed as mean $\pm$ SEM. Student's t test and one-way ANOVA were used for statistical comparisons. A p value <0.05 was used as the criterion for a significant statistical difference.

Acknowledgments

We thank L. Frank and D. Lee for their helpful comments on the manuscript. This work was supported by the Neurobiology Research Program from the KMOST, the KOSEF grant through the Brain Disease Research Center at Ajou University, and the KOSEF-Japan Basic Scientific Promotion Program No. JR090 to M.W.J.

Received: March 3, 2003
Revised: July 7, 2003
Accepted: August 28, 2003
Published: September 24, 2003

References

Baddeley, A. (1986). Working Memory (Oxford: Clarendon press).

Baeg, E.H., Kim, Y.B., Kim, H.T., Mook-Jung, I., and Jung, M.W. (2001). Fast spiking and regular spiking neural correlates of fear conditioning in the medial prefrontal cortex of the rat. Cereb. Cortex *11*, 441–451.

Batuev, A.S., Pirogov, A.A., and Orlov, A.A. (1979). Unit activity of the prefrontal cortex during delayed alternation performance in monkey. Acta Physiol. Acad. Sci. Hung. *53*, 345–353.

Batuev, A.S., Pirogov, A.A., Orlov, A.A., and Sheafer, V.I. (1980). Cortical mechanisms of goal-directed motor acts in the rhesus monkey. In The Warsaw Colloqium on Instrumental Conditioning and Brain Res., B. Zernicki and K. Zielinski, eds. (Warszawa, Poland: Polish Scientific Pub.) pp. 459–481.

Bruce, C.J., Goldberg, M.E., Bushnell, M.C., and Stanton, G.B. (1985). Primate frontal eye fields. II. Physiological and anatomical correlates of electrically evoked eye movements. J. Neurophysiol. *54*, 714–734.

Chang, J.Y., Janak, P.H., and Woodward, D.J. (2000). Neuronal and behavioral correlations in the medial prefrontal cortex and nucleus accumbens during cocaine self-administration by rats. Neuroscience *99*, 433–443.

Constantinidis, C., and Goldman-Rakic, P.S. (2002). Correlated discharges among putative pyramidal neurons and interneurons in the primate prefrontal cortex. J. Neurophysiol. *88*, 3487–3497.

Egorov, A.V., Hamam, B.N., Fransen, E., Hasselmo, M.E., and Alonso, A.A. (2002). Graded persistent activity in entorhinal cortex neurons. Nature *420*, 173–178.

Funahashi, S. (2001). Neuronal mechanisms of executive control by the prefrontal cortex. Neurosci. Res. *39*, 147–165.

Funahashi, S., Bruce, C.J., and Goldman-Rakic, P.S. (1989). Mnemonic coding of visual space in the monkey's dorsolateral prefrontal cortex. J. Neurophysiol. *61*, 331–349.

Funahashi, S., Chafee, M.V., and Goldman-Rakic, P.S. (1993). Prefrontal neuronal activity in rhesus monkeys performing a delayed anti-saccade task. Nature *365*, 753–756.

Fuster, J.M. (1997). The Prefrontal Cortex, Edition 3 (New York: Raven Press).

Fuster, J.M., and Alexander, G.E. (1971). Neuron activity related to short-term memory. Science *173*, 652–654.

Gemmell, C., and O'Mara, S.M. (2000). Long-term potentiation and paired-pulse facilitation in the prelimbic cortex of the rat following stimulation in the contralateral hemisphere in vivo. Exp. Brain Res. *132*, 223–229.

Georgopoulos, A.P., Schwartz, A.B., and Kettner, R.E. (1986). Neuronal population coding of movement direction. Science *233*, 1416–1419.

Goldman-Rakic, P.S. (1995). Cellular basis of working memory. Neuron *14*, 477–485.

Herry, C., Vouima, R.M., and Garcia, R. (1999). Plasticity in the mediodorsal thalamo-prefrontal cortical transmission in behaving mice. J. Neurophysiol. *82*, 2827–2832.

Hirsch, J.C., and Crepel, F. (1990). Use-dependent changes in synaptic efficacy in rat prefrontal neurons in vitro. J. Physiol. *427*, 31–49.

Jog, M.S., Kubota, Y., Connolly, C.I., Hillegaart, V., and Graybiel, A.M. (1999). Building neural representations of habits. Science *286*, 1745–1749.

Jung, M.W., Qin, Y., Barnes, C.A., and McNaughton, B.L. (1998). Firing characteristics of deep layer neurons in prefrontal cortex in rats performing spatial working memory tasks. Cereb. Cortex *8*, 437–450.

Jung, M.W., Qin, Y., Lee, D., and Mook-Jung, I. (2000). Relationship among discharges of neighboring neurons in the rat prefrontal cortex during spatial working memory tasks. J. Neurosci. *20*, 6166–6172.

Kim, M.J., Chun, S.-K., Kim, Y.B., Mook-Jung, I., and Jung, M.W. (2003). Long-term potentiation in visual cortical projections to the medial prefrontal cortex of the rat. Neuroscience *120*, 283–289.

Kolb, B. (1990). Animal models for human PFC-related disorders. Prog. Brain Res. *85*, 501–519.

Kubota, K., and Niki, H. (1971). Prefrontal cortical unit activity and delayed alternation performance in monkeys. J. Neurophysiol. *34*, 337–347.

Laroche, S., Jay, T.M., and Thierry, A.M. (1990). Long-term potentiation in the prefrontal cortex following stimulation of the hippocampal CA1/subicular region. Neurosci. Lett. *114*, 184–190.

Laubach, M., Wessberg, J., and Nicolelis, M.A. (2000). Cortical ensemble activity increasingly predicts behaviour outcomes during learning of a motor task. Nature *405*, 567–571.

Miller, E.K. (1999). The prefrontal cortex: complex neural properties for complex behavior. Neuron *22*, 15–17.

Miller, E.K., and Cohen, J.D. (2001). An integrative theory of prefrontal cortex function. Annu. Rev. Neurosci. *24*, 167–202.

Miller, E.K., Erickson, C.A., and Desimone, R. (1996). Neural mechanisms of visual working memory in prefrontal cortex of the macaque. J. Neurosci. *16*, 5154–5167.

Niki, H., and Watanabe, M. (1976). Prefrontal unit activity and delayed response: relation to cue location versus direction of response. Brain Res. *105*, 79–88.

Oram, M.W., Foldiak, P., Perrett, D.I., and Sengpiel, F. (1998). The 'Ideal Homunculus': decoding neural population signals. Trends Neurosci. *21*, 259–265.

Quintana, J., and Fuster, J.M. (1992). Mnemonic and predictive functions of cortical neurons in a memory task. Neuroreport *3*, 721–724.

Rainer, G., and Miller, E.K. (2000). Effects of visual experience on the representation of objects in the prefrontal cortex. Neuron *27*, 179–189.

Rainer, G., Rao, S.C., and Miller, E.K. (1999). Prospective coding for objects in primate prefrontal cortex. J. Neurosci. *19*, 5493–5505.

Rosner, B. (1995). Fundamentals of Biostatistics, Edition 4 (Belmont, CA: Duxbury Press).

Sutton, R.S., and Barto, A.G. (1998). Reinforcement Learning (Cambridge, MA: MIT Press).

Takeda, K., and Funahashi, S. (2002). Prefrontal task-related activity representing visual cue location or saccade direction in spatial working memory tasks. J. Neurophysiol. *87*, 567–588.

Wang, X.J. (2001). Synaptic reverberation underlying mnemonic persistent activity. Trends Neurosci. *24*, 455–463.

Wilson, M.A., and McNaughton, B.L. (1993). Dynamics of the hippocampal ensemble code for space. Science *261*, 1055–1058.

Zhang, K., Ginzburg, I., McNaughton, B.L., and Sejnowski, T.J. (1998). Interpreting neuronal population activity by reconstruction: unified framework with application to hippocampal place cells. J. Neurophysiol. *79*, 1017–1044.